



**GeoVirtual**  
2020 September  
14-16  
Resilience and Innovation



## Evaluating the Capacity of Helical Piles in Clay Tills Using Pile Load Tests

Ivanna Montani  
*Stantec Consulting Ltd, Winnipeg, Manitoba, Canada*

### ABSTRACT

This thesis analyzes seven static load tests conducted on helical piles installed in clay till at a site in Northern Manitoba, Canada. Four methods, the Davisson Offset Limit, the Hansen Ultimate Load, the Chin-Kondner Extrapolation, and the Decourt Extrapolation are used to determine the ultimate capacity using the pile load test results. The ultimate capacities obtained were then used to determine the empirical parameter  $K_i$  for helical piles in clay tills, this parameter relates the pile capacity of helical piles to the installation torque of the pile. The Davisson Offset Limit and the Hansen Ultimate Load provided consistent and conservative ultimate capacities based on the pile load test results and showed lesser variability in results compared with the Chin-Kondner Extrapolation and Decourt Extrapolation methods. The ultimate loads based from the Hansen and Davisson methods were used to calculate a  $K_i$  value. It was determined that a  $K_i$  value ranging from  $9 \text{ m}^{-1}$  to  $11 \text{ m}^{-1}$  is appropriate for evaluating the capacity of a helical pile in clay tills using the installation torque of the pile.

### RÉSUMÉ

Cette thèse fait l'analyse de sept essais de mise en charge statique effectués sur des pieux vissés installés dans une formation de moraine (till) argileuse dans le nord du Manitoba, au Canada. Quatre méthodes ont été utilisées pour la détermination de la capacité ultime utilisant les résultats des essais de mise en charge : la méthode de la charge limite décalée (Davisson), la méthode de la charge ultime (Hansen), ainsi que les méthodes d'extrapolation de Chin-Kondner et de Decourt. Les capacités ultimes obtenues ont ensuite été utilisées pour déterminer le paramètre empirique  $K_t$  pour pieux vissés en moraine argileuse. Ce paramètre relie la capacité du pieux vissé au couple d'installation du pieu. Les méthodes de la charge limite décalée (Davisson) et de la charge ultime (Hansen) ont fourni des capacités ultimes constantes et conservatrices par rapport aux résultats des essais de mise en charge et ont démontré des résultats moins variables en comparaison avec les méthodes d'extrapolation de Chin-Kondner et de Decourt. Les charges ultimes obtenues à partir des méthodes de Hansen et Davisson ont été utilisées pour calculer une valeur  $K_t$ . Il a été établi qu'une valeur  $K_t$  se situant entre  $9 \text{ m}^{-1}$  et  $11 \text{ m}^{-1}$  est convenable pour l'évaluation de la capacité d'un pieu vissé en moraine argileuse en utilisant le couple d'installation du pieu.

## 1 INTRODUCTION

### 1.1 Objective

This thesis presents and compares four different methods of evaluating the ultimate pile capacity of helical piles from full scale load test data. It determines the parameter that engineers use to estimate the capacity of helical piles. The four methods presented are: the Davisson Offset Limit, the Hansen Ultimate Load, the Chin-Kondner Extrapolation, and the Decourt Extrapolation. These methods were obtained from the Basics of Foundation design book by Bengt H. Fellenius, latest edition published in 2009. Using the ultimate capacities estimated with the four different methods, it is possible to utilize the relationship of helical

load capacity to installation torque recommended in the Canadian Foundations Engineering Manual (CFEM) to determine a range for the empirical parameter,  $K_i$  that engineers use to estimate the capacity of helical piles.

### 1.2 General

Seven helical piles were installed and tested at a site in northern Manitoba. The seven piles are all steel helical piles with an outer shaft diameter ( $d$ ) of 244 millimeters and a single helix located at the toe of the pile with a 457-millimeter diameter ( $D$ ). The piles were installed to a depth ( $H$ ) below the frost sensitive soils line, ranging from 16.71 meters to 18.97 meters below the surface. All piles were installed with the helix embedded in the clay till, below the

frost penetration line. The installation torque ( $T$ ) was recorded for each pile. A schematic for a steel helical pile is provided in Figure 1.

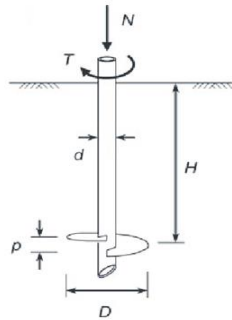


Figure 1. Schematic of Steel Helical Pile (James P. Hambleton, 2014)

The seven pile load tests were conducted following the Quick Method in accordance with ASTM D1143/D1143M-07 (Reapproved 2013) "Standard Test Methods for Deep Foundations Under Static Axial Compressive Load". The static load tests for the piles were limited in deflection as all seven piles were intended to be production piles and later used in construction. For this reason, the tests were not carried to failure. A summary of the dimensions and installation torque for Pile No. 1 through Pile No. 7 is given in Table 1. A summary of all seven Load ( $Q$ ) vs. Deflection ( $\delta$ ) curves from the load test date are shown in Figure 2.

Table 1. Summary of Test Piles

Pile No.	Embedment Below Surface (m)	Shaft Diameter (mm)	Helix Diameter (mm)	Installation Torque (kN-m)
1	16.71	244	457	116
2	18.32	244	457	142
3	18.64	244	457	133
4	18.16	244	457	153
5	17.50	244	457	220
6	18.97	244	457	174
7	16.78	244	457	246

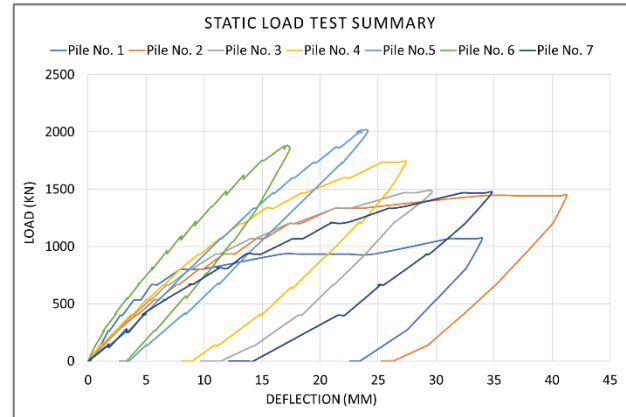


Figure 2. Static Load Test Summary  
1.3 Site Conditions

The test site is located in a region of sporadic discontinuous permafrost. The permafrost was found approximately 10 to 15 meters below the surface, with thaw sensitive soils extending up to 17 meters below the surface. Frozen and thaw sensitive soils may settle upon thawing thereby inducing a drag load (negative skin friction) on the helical piles, for this reason the skin friction capacity of the pile is ignored, and the pile is assumed to derive all its capacity from the bearing resistance of the helix at the toe of the pile. The pre-development site stratigraphy consisted of peat/organic materials followed by a grey clay layer overlying clay till until the end of the boreholes. The peat and organics were observed to be fibrous, wet, and extend from the ground surface to a depth of 1.6 meters. The grey clay layer was observed to be low to medium plasticity, moist, silty and contained some sand and trace gravel. The grey clay layer extends from a depth of 1.6 meters to a depth of 7.4 meters. Clay till was encountered below the clay layer to the depths explored during the geotechnical investigation. The clay till was grey and low in plasticity, contained silt, some sand, and gravel. The clay till was confirmed to be very dense in compactness through Standard Penetration Test (SPT) at the site.

## 2 LITERATURE REVIEW

### 2.1 Helical Piles

Steel helical piles, also known as screw piles or screw anchors, are a type of deep foundation used to provide stability against compressive, tensile, and lateral loads for a structure (Tappenden & Segio, 2007). A screw pile consists of a circular pile shaft with one or more helices attached to the shaft of the pile by welding to increase the bearing capacity of pile. Due to their varying sizes helical piles may be used for a variety of applications with a wide range of loading scenarios ranging from large piles to support bridges and lighthouses to smaller piles used as foundations for cabins and decks (Koulack, 2016). Helical piles are installed by screwing the pile into the ground by applying a turning moment at the head of the pile which causes the helices to penetrate the ground (Tappenden &

Sego, 2007). There are several methods of installation depending on the size of the pile and the soil in which it is being installed. Smaller piles are installed using a manually powered wrench while larger piles are installed with a hydraulic wrench (Koulack, 2016). Figure 3 shows an example of helical pile installation with a hydraulic wrench.



Figure 3. Helical Pile Installation with Hydraulic Wrench (courtesy of Stantec Consulting Ltd.)

Installation for helical piles usually requires minimal to no excavation which makes this foundation type well suited for installation near other structures, as well they are a quick and economical option where no delay in construction is important (Koulack, 2016). Screw piles are not typically well-suited for installation in very dense gravelly soils that may cause damage to the helices or have shallow refusal, but there has been commercial screw piles fabricated with thick helices, up to 25 mm, to prevent damage during installation in dense soils (Tappenden & Sego, 2007).

## 2.2 Static Load Testing

A static load test is conducted by applying a load to an installed pile and measuring the movement, or deflection of the pile at the applied load. A static load test is a method of verifying the predicted ultimate capacity of a pile. Axial compression static load tests in Canada must be conducted in accordance with ASTM D1143/D1143M-07 (Reapproved 2013). Within this standard there are several methods of conducting load tests. The load test data analyzed in this paper was obtained through the “Quick Load Test Method”. This test is conducted by applying small load increments at short time intervals, the test is

usually carried to failure or a predetermined maximum load and typically lasts 3 to 6 hours (CFEM, 2006). For this test method, the duration of each load increment should not exceed 15 minutes and should not be shorter than 5 minutes. It is recommended that the load increments to failure or maximum predetermined load should not be less than 25 increments, 35 to 40 preferred (CFEM, 2006). Figure 4 below provides a schematic for a typical static load test set up.

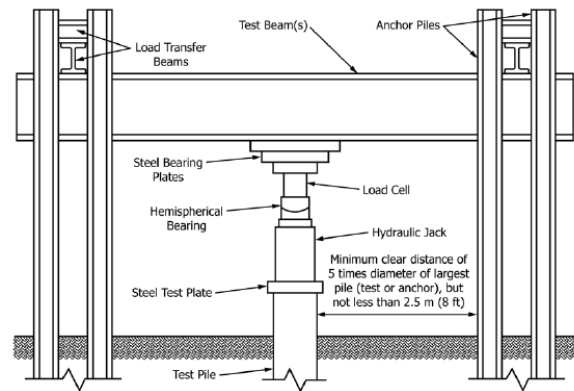


Figure 4. Schematic of Hydraulic Jack Acting Against Anchored Reaction Frame (ASTM Designation: D1143/D1143M-07, 2013)

A typical static load test is composed of the pile being tested, a load cell that applies the load to the test pile, as well as a load transfer beam and anchor piles that hold the system in place as the load is applied. Four dial gauges are used to measure the pile head deflection measured relative to a fixed reference beam, the average of the four readings is the used for the load-deflection curve.

## 2.3 Pile Capacity

The design capacity of a foundation element, such as a pile, communicated to the structural engineer is determined by applying a resistance factor to an ultimate capacity value. The ultimate pile capacity can be predicted using theoretical methods and is verified by interpreting the pile capacity from the static load test of the pile or using the installation torque and capacity relationship.

Static load testing is a method of measuring the capacity of a pile, this is important to do for pile foundation projects in order to confirm the capacity and verify if the field performance of the pile agrees with that assumed in the design (Fellenius, 2009). The ultimate capacity of a pile is determined using the load-deflection curve from a static load test. A very simple way to define failure using this relationship is ‘plunging failure’. Plunging failure occurs when rapid deflection of the pile occurs under a sustained load or a slight increase of the applied load (Fellenius, 2009). It is arguable that this definition of failure is not adequate, in most cases large deflections are required for plunging failure to occur. This does not often happen during testing and therefore the pile capacity or ultimate load must

be determined by a definition based on the load-deflection data from the test (Fellenius, 2009).

Terzaghi once defined the definition of capacity to be the load for which a pile head movement, or deflection, exceeds 10% of the diameter of that pile. This definition does not consider the elastic shortening of the pile during loading. In practice movement limits are typically related to the tolerance of movement by the superstructure to be supported by the pile, defined by serviceability limits, this movement does not relate to the capacity of a pile as a soil response to the loads applied in the static load test (Fellenius, 2009).

Another definition of pile capacity is the intersection of two lines on the static load test load-deflection curve, one straight line approximates the pseudo-elastic behavior of the line while the other the pseudo-plastic behavior (Fellenius, 2009). The capacity interpreted using this method can vary greatly depending on judgement and on the scale of the graph. If the scale of the graph is changed, the perceived capacity for the pile may also change. While the interpretation of a loading test may be influenced by many factors, the scale of the graph should not be one of them (Fellenius, 2009). It is important to provide a proper definition of pile capacity to give meaning to the interpretation of pile load tests, a definition based on a mathematical rule that will generate values independent of drafting, judgement, or the ability of the individual interpreter. The definition of pile capacity must consider the load-deflection curve of the pile, or the length of the pile (Fellenius, 2009).

An estimate of helical pile capacity can be obtained through monitoring of the installation torque for the pile. Recording and monitoring the installation torque of the pile can also be used as a quality control method. Piles that do not achieve the required installation torque predetermined by the design engineer may require load testing (CFEM, 2006). The parameter  $K_t$  is used as a relationship between the load capacity and installation torque of a pile and can be used to verify that a helical pile has reached its predicted capacity.

## 2.4 Methods of Evaluating Pile Capacity

The following our methods were used to evaluate the capacity of the piles from the static load test results.

### 2.4.1 Davisson Offset Limit

This method, developed by Davisson in 1972, defines the limit load corresponding to the movement which exceeds elastic compression of the pile by a value of 4 millimeters plus a factor equal to the diameter of the pile divided by 120 (Fellenius, 2009). It should be noted that the offset limit load is not necessarily the ultimate load. This method assumes that the capacity of the pile is reached at a certain small toe movement. It tries to estimate that movement by compensating for the stiffness, that is the length and diameter, of the pile (Fellenius, 2009). This method was developed by correlating subjectively-considered pile-capacity values for many pile loading tests to a single criterion. The primary intention for this method is for driven piles tested according to quick methods (Fellenius, 2009).

### 2.4.2 The Hansen Ultimate Load

The Hansen Ultimate Load method was proposed by Hansen in 1963 and defines the capacity of a pile as “the load that gives four times the movement of the pile head as obtained for 80% of that load” (Fellenius, 2009). The Hansen 80% criterion is said to agree well with the intuitively perceived plunging failure (Fellenius, 2009). This method is a curve fitting method, the Hansen curve is developed using curve fitting coefficients obtained from the load-deflection data of the load test. To apply this method, square root each deflection value and divide it by its corresponding load, then plot that value by the deflection (Fellenius, 2009). The curve fitting coefficients are obtained from the slope and y-intercept of this graph. The coefficients can then be used to plot the Hansen curve and calculate the Hansen Ultimate Load.

### 2.4.3 Chin-Kondner Extrapolation

This method was developed by Chin in 1970-1971, extending the work by Kondner in 1963. The Chin-Kondner Extrapolation is similar to the Hansen method in that it is a curve fitting method. To apply this method, each deflection is divided by its corresponding load and the resulting value is plotted against the deflection (Fellenius, 2009). Typically, there is some initial variation but eventually the values fall on straight line. The curve fitting coefficients are obtained from the slope of the straight line and the y-intercept of the straight line. The coefficients are used to develop the Hansen curve, and calculate the ultimate capacity. This ultimate load is approached asymptotically, for that reason the ultimate load value calculated using the Chin-Kondner Extrapolation method is typically higher than the actual ultimate load obtained from the load test curve. Fellenius explains that it is a sound engineering rule never to interpret the results from a static loading test to an ultimate load larger than the maximum load applied to the pile in the test (Fellenius, 2009). This statement refers to tests performed to failure. However, one cannot determine the allowable load from the test by simply applying a resistance factor in this case. The Chin-Kondner extrapolation is better used during the progress of a static load test to assess the quality of the test (Fellenius, 2009). For example, if a weakness in the pile should develop during the test, the Chin-Kondner extrapolation shows a kink in the plot (Fellenius, 2009). For this reason, this method is best used by plotting the readings with the Chin-Kondner as the test progresses. It is valuable to compare the results of this method to the methods of the Davisson and Hansen (Fellenius, 2009).

### 2.4.4 Decourt Extrapolation

The Decourt Extrapolation method was developed by Decourt in 1999 and it the most recent of the methods explored in this study. This method is very similar to the Hansen and Chin-Kondner methods. It also uses curve fitting to estimate the ultimate capacity of the tested pile. To apply this method, one must divide each load with its corresponding deflection and plot the resulting value

against the applied load. The straight line that develops from this graph can then be used to obtain the curve fitting coefficients to develop the Decourt Extrapolation curve and obtain the ultimate load. There is an advantage in preparing the indicated plot while the static load test is in progress. It allows the user to 'eyeball' the ultimate capacity of the pile once a straight line starts to develop (Fellenius, 2009).

### 3 METHODOLOGY

#### 3.1 Evaluating Ultimate Capacity

The seven static load tests analyzed were not performed to failure, because the piles tested were used for construction. This thesis attempts to estimate the ultimate capacity of these seven piles using predictive methods described in Chapter 8 of "The Basics of Foundation Design" by Bengt H. Fellenius. The four methods explored are the Davisson Offset Limit, the Hansen Ultimate Load, the Chin-Kondner Extrapolation, and the Decourt Extrapolation method. The methods are described in the sections below.

##### 3.1.1 Davisson Offset Limit

The offset limit is obtained by plotting the elastic deflection line and offsetting it by the offset value provided from the literature in SI units, shown in Equation 1.

$$\text{Offset (SI Units)} = 4 \text{ mm} + \frac{b}{120} \quad [1]$$

Where:

b = pile diameter (in this case, helix diameter of 457 mm)

The equation of the elastic line was obtained from the load test data using the unloading curve, which theoretically has the same slope as the elastic loading curve. An example for obtaining the slope of the elastic curve using the load test data for Pile No. 4 is shown in Figure 5 **Error! Reference source not found.**

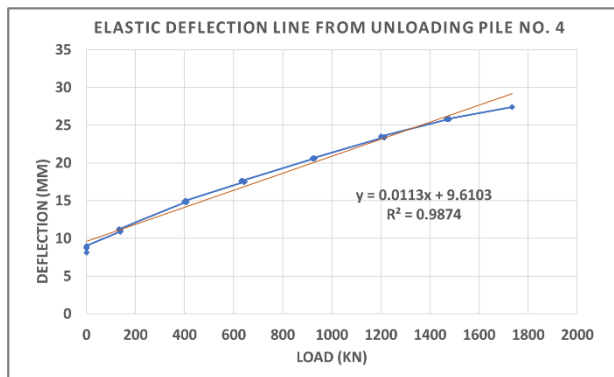


Figure 5. Slope of Elastic Curve

This slope is multiplied by the load applied to the pile to obtain the elastic deflection line. The Davisson offset limit is then applied to the elastic deflection ( $\delta_{elastic}$ ) line as shown in the Equation 2 and 3 below.

$$\delta_{elastic} = (Q_{applied}) * (0.0113) \quad [2]$$

$$\text{Offset Limit Line} = \delta_{elastic} + \left(4\text{mm} + \frac{b}{120}\right) \quad [3]$$

Where:

b = 457 mm

The Davisson offset limit line can then be plotted against the load-deflection line for the Pile No.4 load test, the intersection of the lines is then described as the Davisson Offset Limit. In this case we use this limit as the ultimate capacity of the pile undergoing testing. Figure 6 shows the results for the Pile No. 4 static load test with the superimposed offset limit.



Figure 6. Davisson Offset Limit, Pile No. 4

If a pile does not undergo sufficient deflection during load testing, the load-deflection curve will not reach the Davisson Offset Limit, this is one of the limitations of this method. Figure 7 below shows the load-deflection curve for Pile No. 5, this pile experienced very little deflection during testing, for this reason the Davisson Offset Limit did not apply. Summary tables and graphs for the application of the Davisson Offset Limit method for the load tests of Pile No. 1 through Pile No. 7 are provided in Appendix A.

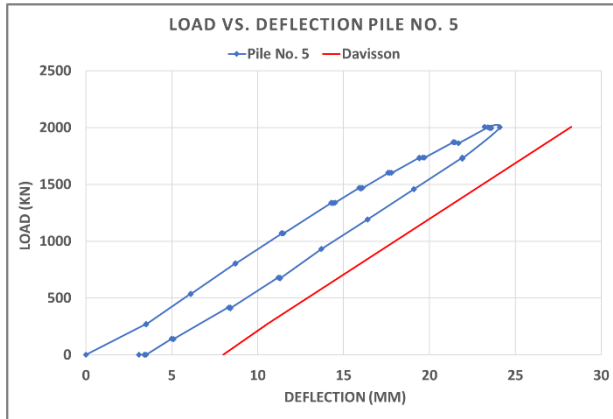


Figure 7. Davisson Offset Limit, Pile No. 5

### 3.1.2 The Hansen Ultimate Load

The 80% criterion for the Hansen Ultimate Load can be estimated from the load-deflection curve, but it is more accurate to plot the square root of each deflection value divided by its load value, and plot it against the deflection, as shown in Equation 4.

$$\frac{\sqrt{\delta}}{Q} \text{ vs. } \delta \quad [4]$$

The plot provides a curve that tends towards a straight line, using a trendline we can define the  $C_1$  and  $C_2$  curve fitting coefficients to develop the Hansen curve. The  $C_1$  coefficient is the slope of the straight line developed, and the  $C_2$  coefficient is the y-intercept of the straight line. Figure 8 shows the plot used to develop the  $C_1$  and  $C_2$  coefficients for Pile No. 2 using the Hansen method.

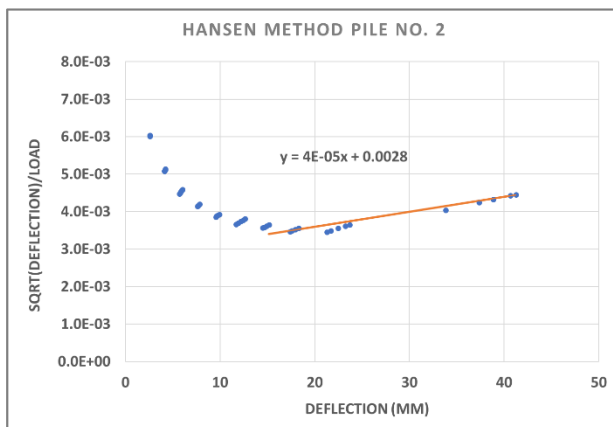


Figure 8. Pile No. 2 Plot to Obtain Curve Fitting Coefficients

With the coefficients obtained from the straight line in the figure above it is now possible to get the Hansen curve using Equation 5 from the literature and plot it against the load-deflection curve from the test data.

$$Q = \frac{\sqrt{\delta}}{C_1\delta + C_2} \quad [5]$$

Figure 9 shows the Hansen curve developed from the Pile No. 2 load test data with the equation above, superimposed with the load-deflection curve from the test data.

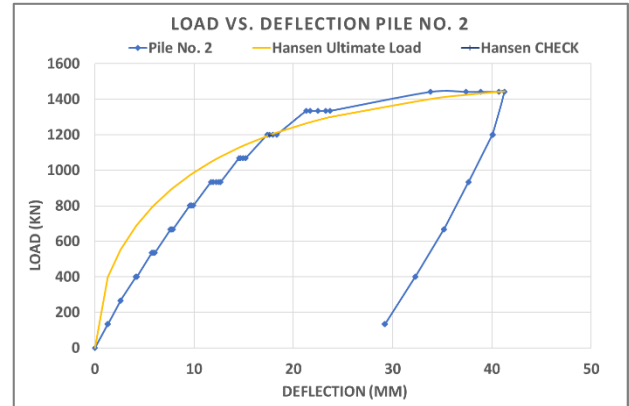


Figure 9. Hansen Curve for Pile No. 2

The Hansen Ultimate Load and the deflection at this load can then be determined using Equation 6 and 7 respectively.

$$Q_u = \frac{1}{2\sqrt{C_1 C_2}} \quad [6]$$

$$\delta_u = \frac{C_1}{C_2} \quad [7]$$

For this method, it is important to check the point  $0.80Q_u/0.25\delta_u$ . This point should lie on or near the measured load-deflection curve. The relevance of this method can be determined by superimposing the load-deflection curve and the Hansen curve. Both curves should be near the load equal to about 80% of the Hansen ultimate load and the ultimate load itself (Fellenius, 2009). Summary tables and graphs for the application of the Hansen Ultimate Load method for the load tests of Pile No. 1 through Pile No. 7 are provided in Appendix A.

### 3.1.3 Chin-Konder Extrapolation

To apply this method, each deflection is divided by its corresponding load and plotting the resulting value against the deflection. Typically, there is some initial variation but eventually the values fall on a straight line. A trendline of this straight line can provide the trend fitting coefficients for

this method,  $C_1$  the slope of the straight line, and  $C_2$  the y-intercept of the straight line (Fellenius, 2009). Figure 10 shows the plot used to get the curve fitting coefficients for Pile No. 4.

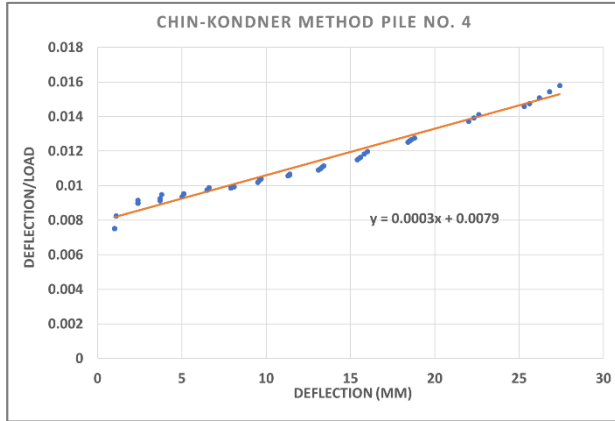


Figure 10. Chin Kondner Straight Line Graph

Using the curve fitting coefficients  $C_1$  and  $C_2$  and Equation 8, the Chin-Kondner extrapolation loads can be calculated as follows:

$$Q = \frac{\delta}{C_1\delta + C_2} \quad [8]$$

The Chin-Kondner loads can then be plotted against the deflection to create the Chin-Kondner Extrapolation curve. This plot is superimposed with the load-deflection curve from the test results to evaluate the fit of the Chin-Kondner Extrapolation curve against the load test data. Both the load-deflection curve and the Chin-Kondner Extrapolation curve for Pile No. 4 are shown in Figure 11.

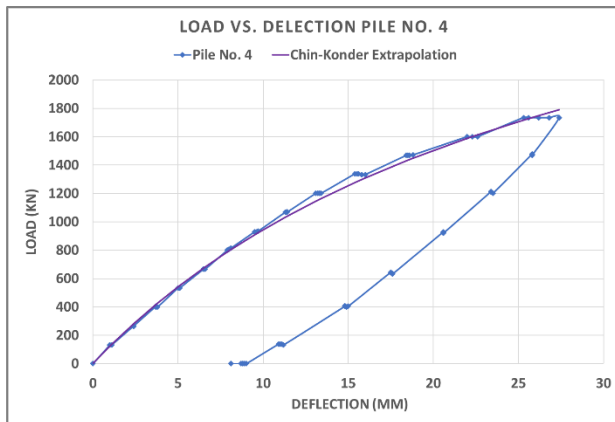


Figure 111. Chin-Kondner Extrapolation Curve for Pile No. 4

The ultimate load as described by the Chin-Kondner Extrapolation method is calculated using Equation 9:

$$Q_u = \frac{1}{C_1} \quad [9]$$

This ultimate load is approached asymptotically, for that reason the ultimate load value calculated using the Chin-Kondner Extrapolation method is typically higher than the actual ultimate load obtained from the load test curve.

With regards to the limitations to the Chin-Kondner method, typically the correct straight line is not achieved until the test load has passed the Davisson Offset Limit. This may produce an incorrect ultimate load if the method is applied too early in the test, or the pile undergoes small deflections. A general rule is that the Chin-Kondner Extrapolation load should be approximately 20% to 40% greater than the Davisson Limit (Fellenius, 2009). Summary tables and graphs for the application of the Chin-Kondner Extrapolation for the load tests of Pile No. 1 through Pile No. 7 are provided in Appendix A.

### 3.1.4 Decourt Extrapolation

To apply this method, one must divide each load with its corresponding deflection and plot the resulting value against the applied load. Figure 12 shows the Decourt straight line graph for Pile No. 2.

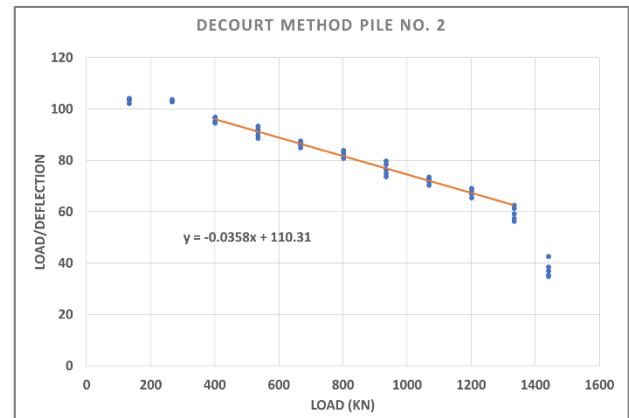


Figure 122. Decourt Extrapolation Straight Line

From the linear regression over the apparent line the coefficients  $C_1$  and  $C_2$  can be obtained as the slope of the straight line and the y-intercept of the straight line respectively. Using the coefficients, it is possible to generate an "ideal" curve using Equation 10.

$$Q = \frac{C_2\delta}{1 - C_1\delta} \quad [10]$$

Figure 13 shows the Decourt Extrapolation Curve plotted against the load test results for Pile No. 2.

$$K_t = \frac{Q_u}{T} \quad [13]$$

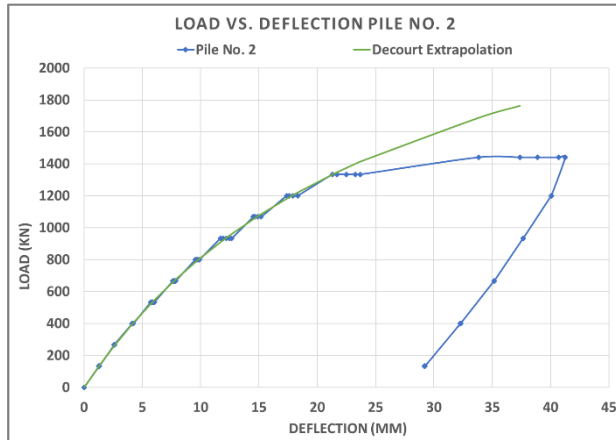


Figure 133. Decourt Extrapolation Curve for Pile No. 4

The Decourt Extrapolation ultimate load can then be determined using Equation 11.

$$Q_u = \frac{C_2}{C_1} \quad [11]$$

The results from the Decourt Extrapolation are similar to those obtained using the Chin-Kondner method. Summary tables and graphs for the application of the Decourt Extrapolation method for the load tests of Pile No. 1 through Pile No. 7 are provided in Appendix A.

### 3.2 Determining the Parameter $K_t$

The ultimate capacity of helical piles can be estimated using the installation torque of the pile. A relationship between the load capacity and installation torque was developed. Equation 12 shows the relationship which relates the ultimate capacity of the pile  $Q_u$  with the installation torque of the pile ( $T$ ) using the empirical torque factor,  $K_t$  (CFEM, 2006).

$$Q_u = K_t * T \quad [12]$$

The value for  $K_t$  from the Canadian Foundation Engineering manual ranges from  $10 \text{ m}^{-1}$  to  $33 \text{ m}^{-1}$  if the torque is recorded in Newton-meters (N-m). For shaft diameters approaching 200 millimeters the recommended  $K_t$  value is  $10 \text{ m}^{-1}$  (CFEM, 2006). Equation 12 can be arranged to provide a formula for obtaining  $K_t$  using the ultimate capacities predicted with each method as shown in Equation 13.

The resulting  $K_t$  values can then be analyzed to determine an appropriate value to be used for helical piles in clay tills, as well as to validate the literature value of  $K_t = 10/\text{m}$ .

## 4 RESULTS AND DISCUSSION

### 4.1 Evaluating Ultimate Capacity

Summary graphs for each pile load test for Pile No. 1 through Pile No. 7 showing all the methods applied plotted against the load-deflection curve are provided in Appendix B. The ultimate capacity determined for each pile using the different methods is shown in Figure 14, as well as tabulated in Table 2 below.

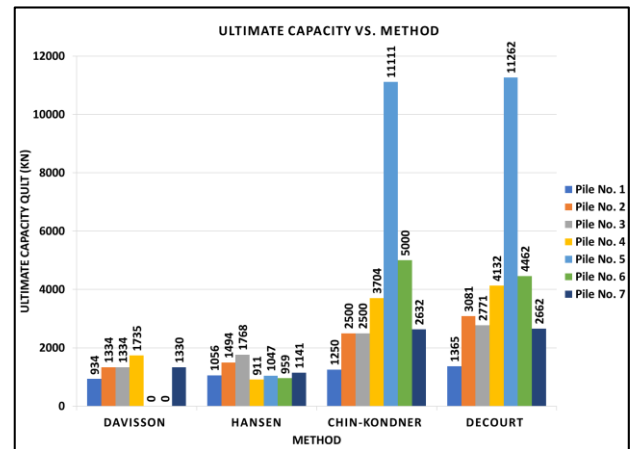


Figure 144. Ultimate Capacity Analysis Results

Table 2. Summary of Ultimate Capacity Estimates

Pile No.	Ultimate Load Estimated (kN)				Max Applied Load (kN)
	Davisson	Hansen	Chin-Kondner	Decourt	
1	934	1,056	1,250	1,365	1,068
2	1,334	1,494	2,500	3,081	1,441
3	1,334	1,768	2,500	2,771	1,468
4	1,735	911	3,704	4,132	1,735
5	N/A	1,047	11,111	11,262	2,006
6	N/A	959	5,000	4,462	1,882
7	1,330	1,141	2,632	2,662	1,468

It is apparent from looking at Figure 14 that the Davisson Offset Limit and the Hansen Ultimate Load methods provide more consistent results in comparison to the Chin-Kondner Extrapolation and the Decourt



Extrapolation. The estimated ultimate capacities for the Davisson method range from 934 kN to 1,735 kN with Pile No. 5, and Pile No. 6 displaying no ultimate capacity values due to not having enough deflection to reach the Davisson Offset Limit.

The ultimate loads evaluated with the Hansen method ranged from 911 kN to 1,768 kN, very similar values to the Davisson method. For some piles the ultimate value determined by this method is higher than the maximum applied load during testing. Note again that the pile load tests selected for this analysis were not carried to failure of the pile. For this reason, it is understandable to obtain a capacity larger than the maximum applied load for the pile.

The Hansen check of plotting the  $0.80Q_u/0.25\delta_u$  point to verify that it lies near or on the Hansen curve was performed for all the piles load tests and can be seen plotted in the summary graphs provided in Appendix A. The Hansen check point does not often lie on the curve for the data analyzed. This could be due to the deflections experienced by most piles during testing is relatively small compared to the deflections that would have been experienced if the tests were conducted to failure. This assumption is further reinforced by comparing the Hansen curve and test load-deflection curves for those piles that did undergo large deflections. Specifically Pile No. 1 and Pile No. 2, these piles show the  $0.80Q_u/0.25\delta_u$  Hansen check point lies directly on the curve. Another criterion from the literature to confirm the validity of the Hansen method is that both curves should be near the load equal to about 80% of the Hansen ultimate load and the ultimate load itself, from the summary graphs it can be observed that the Hansen Ultimate Load curve and the load-deflection curve from testing converge towards higher loads.

The Chin-Kondner Extrapolation method for determining ultimate capacity estimates range from 1,250 kN to 3,704 kN with Pile No. 5 and Pile No. 6 as obvious outliers with ultimate capacities of 11,111 kN and 5,000 kN respectively. All the ultimate capacities estimated by the Chin-Kondner method are higher than the maximum applied load during testing, while it has been noted repeatedly that the tests analyzed in this paper were not carried to failure, the literature (Fellenius, 2009) warns that the Chin-Kondner method yields ultimate pile capacities higher than the maximum applied load during testing due to its asymptotic nature. It is likely that the straight line for this method did not properly develop for Pile No. 5 and Pile No. 6 due to low deflections experienced during testing.

The Decourt Extrapolation values for estimated ultimate capacity ranged from 1,365 kN to 4,462 kN with Pile No. 5 as an obvious outlier with a predicted ultimate capacity of 11,262 kN, these values were very similar to those produced by the Chin-Kondner method. It is likely that the reason for the variability in capacities using this method lies within the same reasoning for the variability in the Chin-Kondner method.

The approximate ultimate capacity for a helical pile commonly used in a clay till soils is within the 1,000 kN to 2,000 kN range. Therefore, it is reasonable to say that the Davisson and Hansen methods provide more realistic, and conservative values for ultimate capacity. The Chin-Kondner and Decourt methods provide more variable

ultimate capacities for these seven piles than the first two methods, with Pile No. 5 and Pile No. 6 considered as outliers. While the Chin-Kondner and Decourt methods showed less consistent results than the first two methods, it is worth noting that the Chin-Kondner and Decourt curves followed the behavior of the load-deflection curve very closely. This lends itself to the idea that if the load tests for the seven piles were performed to failure these methods may have produced more accurate results. Summary graphs for each pile load test for Pile No. 1 through Pile No. 7 showing all the methods applied plotted against the load-deflection curve are provided in Appendix B.

#### 4.1.1 Determining Parameter $K_t$

The empirical torque factor  $K_t$  is used to provide an estimate of the ultimate capacity of a helical pile using the installation torque of the pile. In this case, the estimated ultimate capacity values from each method were used to determine  $K_t$  for each method and evaluate an appropriate  $K_t$  value for helical piles in clay tills. Figure 15 shows a plot of  $K_t$  determined from the ultimate load obtained from each method, for each pile.

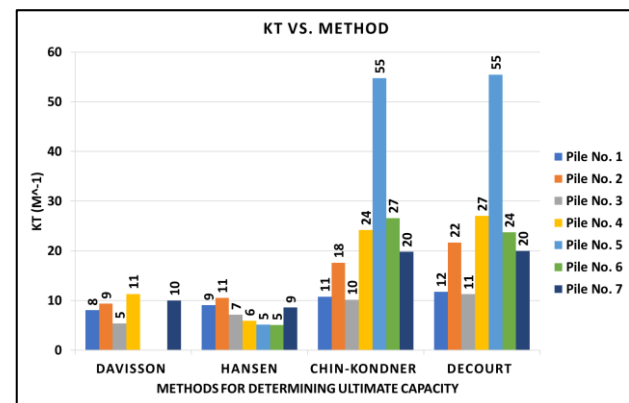


Figure 155. Summary of  $K_t$  Values for Each Method

As discussed previously, the ultimate values for the Chin-Kondner and Decourt methods varied and were generally higher than expected. Therefore, the values for  $K_t$  calculated from the ultimate capacities from this method are also quite variable and higher than expected. For this reason, the focus will remain on the Davisson method and the Hansen method. The Davisson ultimate capacities produced  $K_t$  values ranging from  $5\text{ m}^{-1}$  to  $11\text{ m}^{-1}$ , with an average  $K_t$  value of  $9\text{ m}^{-1}$ . Piles 5 and 6 are not included in this average being considered as outliers. The Hansen ultimate capacities produced  $K_t$  values from ranging from  $5\text{ m}^{-1}$  to  $11\text{ m}^{-1}$ , with an average  $K_t$  of  $7\text{ m}^{-1}$ , all piles are included in this average. It is therefore adequate to assume that a  $K_t$  range of  $9\text{ m}^{-1}$  to  $11\text{ m}^{-1}$  is acceptable for use for predicting the ultimate capacity of a helical pile in clay tills. This agrees with the literature value of  $10\text{ m}^{-1}$  from the Canadian Foundations Engineering Manual (CFEM).

## 5 SUMMARY AND CONCLUSION

Seven helical piles underwent static load testing at a site in northern Manitoba. The piles were installed in an area of sporadic discontinuous permafrost with thaw sensitive soils encountered to a depth of up to 17 m. Due to the downdrag that may be induced on the piles by the thaw sensitive soils, the portion of the pile capacity derived from skin friction was ignored and the entire capacity of the pile is derived from the toe bearing capacity. The seven piles tested at this site were production piles, later to be used for construction. Therefore, for the piles to meet serviceability criteria for construction the tests were not loaded to failure.

This thesis presented and compared four different methods of evaluating the ultimate pile capacity of a pile from full scale load test data for the seven piles. The four methods used to evaluate pile capacity are: the Davisson Offset Limit, the Hansen Ultimate Load, the Chin-Kondner Extrapolation, and the Decourt Extrapolation. Using the ultimate capacities estimated with the four different methods and the relationship of helical load capacity to installation torque from the Canadian Foundations Engineering Manual (CFEM) it was possible to determine a range for the empirical parameter  $K_t$  that engineers can use to estimate the capacity of helical piles using the installation torque in clay tills.

Ultimately, after the analysis of the four methods for each of the seven load tests it was found that the Davisson Offset Limit and the Hansen Ultimate Load methods provide reasonable and less variable ultimate pile capacities within the expected range of 1000 kN to 2000 kN for helical piles in clay tills. These two methods were consistent with each other as well as overall conservative estimates in comparison with the other two methods that have also been evaluated. It must be noted that the Davisson Ultimate load did not apply for piles that experience small deflections and do not intersect the Davisson offset line, such scenarios were observed for Pile No. 5 and Pile No. 6. It may also be for this reason that the Chin-Kondner and the Decourt Extrapolation methods produced very high estimated capacities for these two piles. A limitation of the Chin-Kondner method is that the correct straight line for this method typically does not materialize until the Davisson Offset Limit is reached. It is important to note that all four methods for analyzing the ultimate capacity of a pile from load test data should be always considered and compared to provide meaningful results and a valuable conclusion.

Using the range of ultimate capacities estimated using the Davisson Offset Limit and the Hansen Ultimate Load methods, and the relationship between the installation torque and the ultimate capacity, an appropriate range for  $K_t$  was developed. It was determined based on the results from the Hansen and Davisson methods that a range of  $K_t$  from  $9 \text{ m}^{-1}$  to  $11 \text{ m}^{-1}$  are suitable for the prediction of ultimate capacity of helical piles installed in clay tills. This range agrees well with the recommended value of  $10 \text{ m}^{-1}$  from the CFEM. It should be noted that only seven pile load tests were analyzed, and the analysis of more pile load tests in a similar soil conditions will help refine the suitable value for  $K_t$ .

## REFERENCES

- ASTM Designation: D1143/D1143M-07. (2013). Standard Test Methods for Deep Foundations Under Static Axial Compressive Load. American Society for Testing and Materials (ASTM). West Conshohocken, PA: ASTM International.
- CFEM. (2006). Canadian Foundation Engineering Manual 4th ed. Richmond British Columbia: The Canadian Geotechnical Society.
- Fellenius, B. H. (2009). Basics of Foundation Design. Sidney, BC: www.fellenius.ca.
- James P. Hambleton, S. S. (2014, December). ResearchGate. Retrieved from Analysis of Installation of Helical Piles in Clay: [https://www.researchgate.net/figure/Schematic-of-a-deeply-embedded-helical-pile-with-a-single-helical-plate-a-installation\\_fig1\\_271508701](https://www.researchgate.net/figure/Schematic-of-a-deeply-embedded-helical-pile-with-a-single-helical-plate-a-installation_fig1_271508701)
- Koulack, E. (2016). Axial Compressive Capacity of Helical Piles with Floating Stabilizer in Winnipeg Clay. GeoVancouver2016. Vancouver: Canadian Geotechnical Society.
- Tappenden, K. M., & Segoo, D. C. (2007). Predicting the Axial Capacity of Screw Piles Installed in Canadian Soils. OttawaGeo2007 (pp. 1608-1615). Ottawa: Canadian Geotechnical Society.

## APPENDIX A

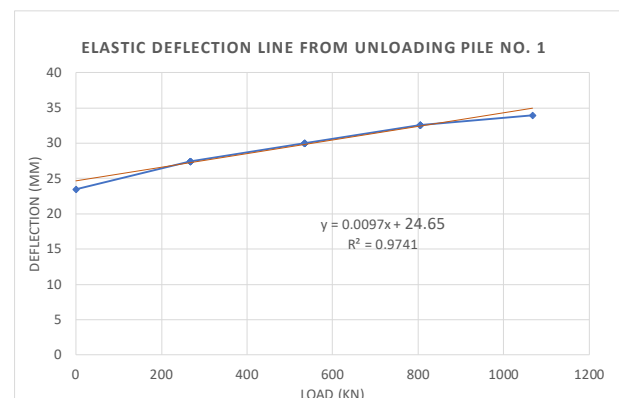


Figure A1. Davisson Offset Limit Method Pile No. 1

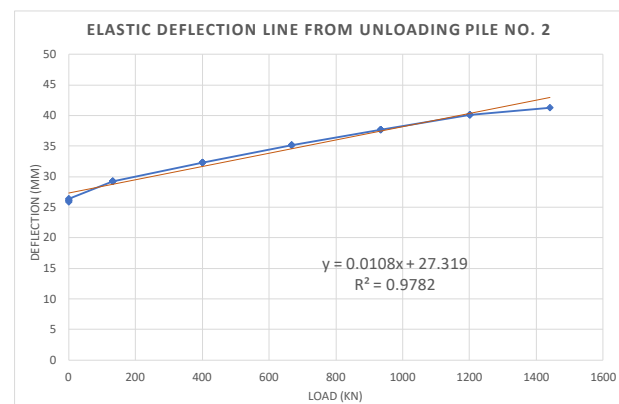


Figure A2. Davisson Offset Limit Method Pile No. 2

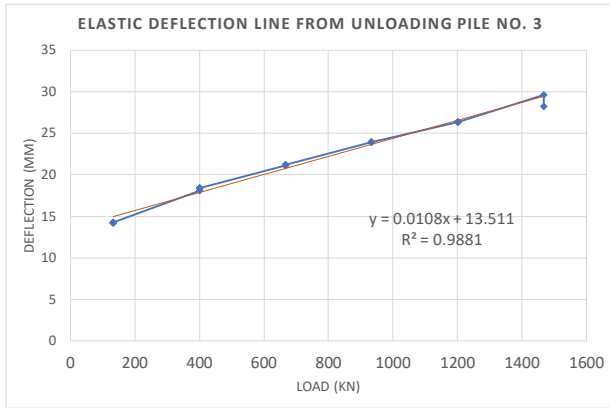


Figure A3. Davisson Offset Limit Method Pile No. 3

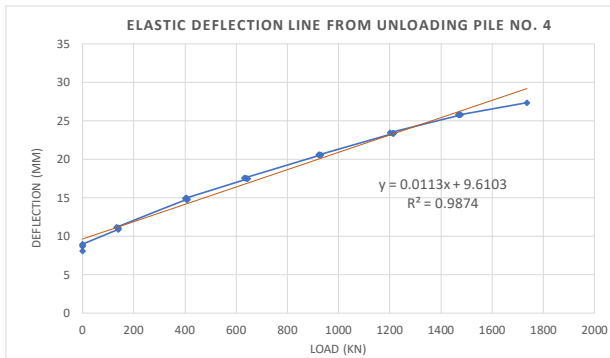


Figure A4. Davisson Offset Limit Method Pile No. 4

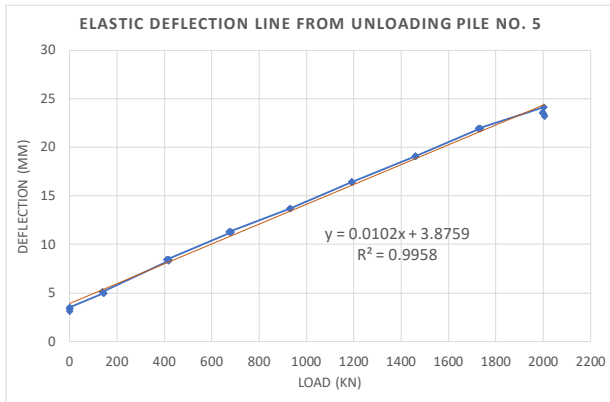


Figure A5. Davisson Offset Limit Method Pile No. 5

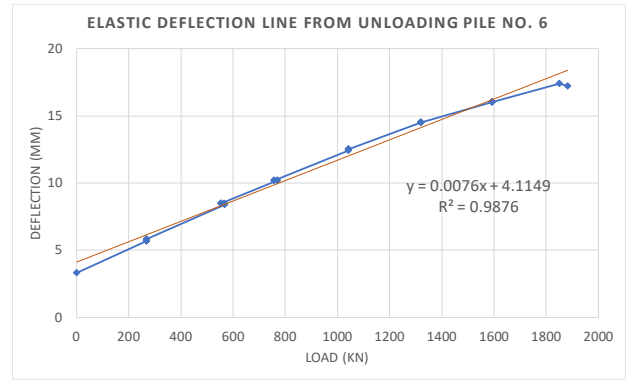


Figure A6. Davisson Offset Limit Method Pile No. 6

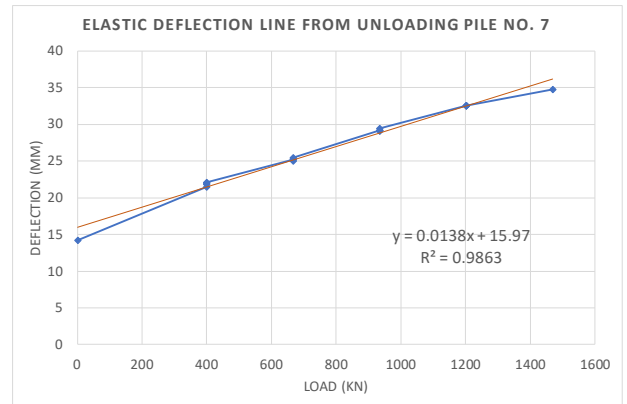


Figure A7. Davisson Offset Limit Method Pile No. 7

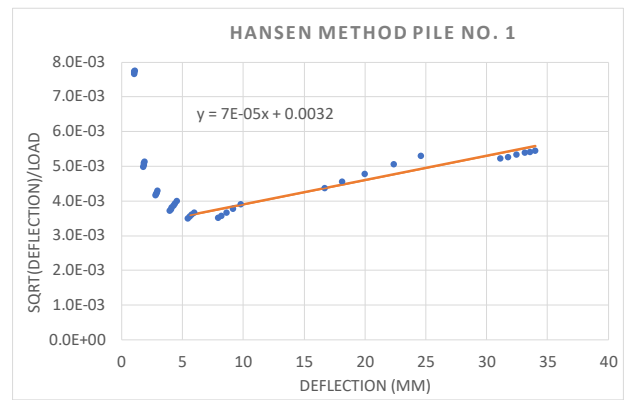


Figure A8. Hansen Ultimate Load Method Pile No.1

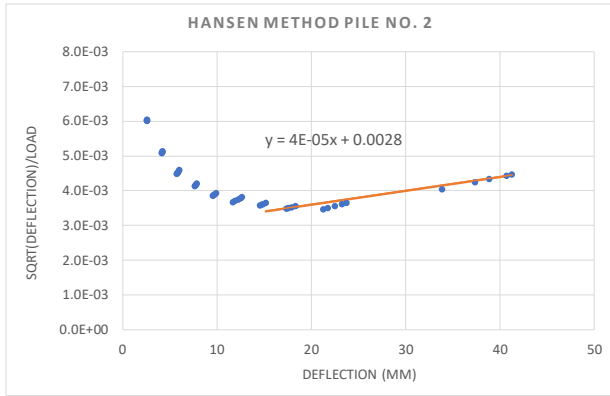


Figure A9. Hansen Ultimate Load Method Pile No.2

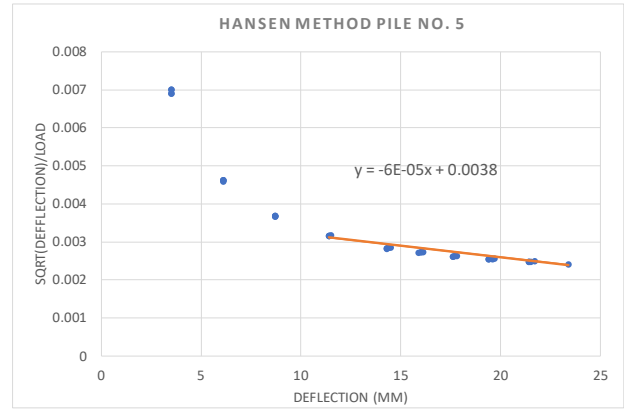


Figure A12. Hansen Ultimate Load Method Pile No.5

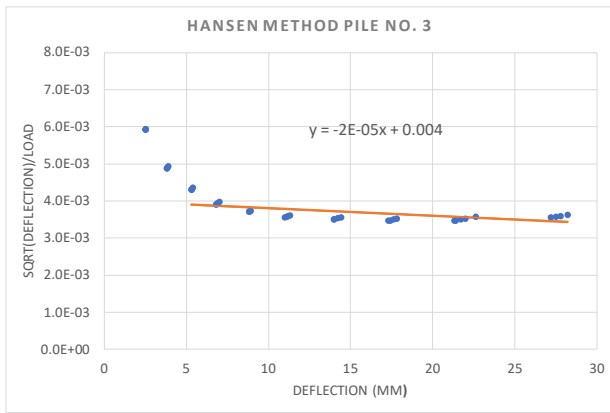


Figure A10. Hansen Ultimate Load Method Pile No.3

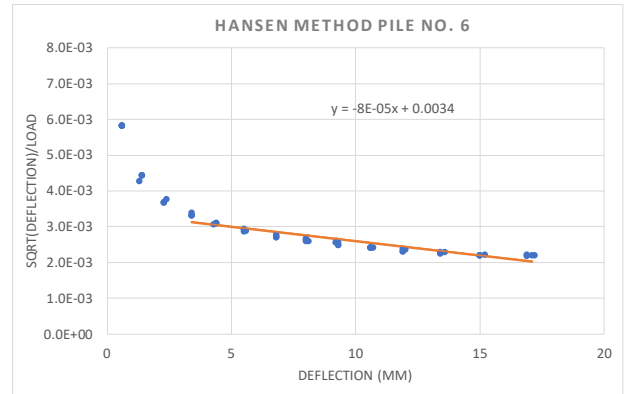


Figure A13. Hansen Ultimate Load Method Pile No.6

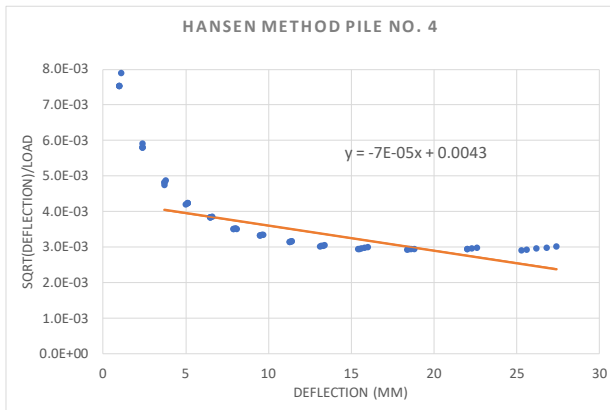


Figure A11. Hansen Ultimate Load Method Pile No.4

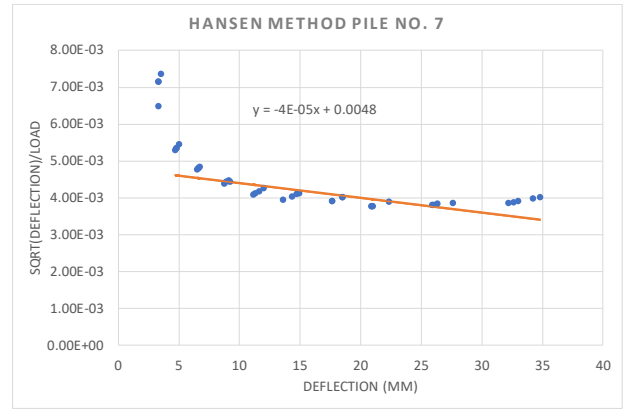


Figure A14. Hansen Ultimate Load Method Pile No.7

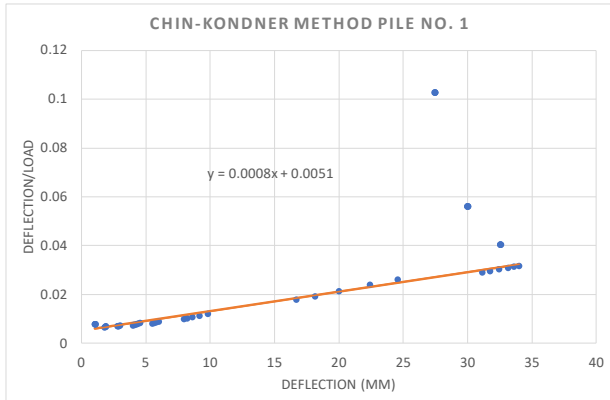


Figure A15. Chin-Kondner Extrapolation Method Pile No. 1

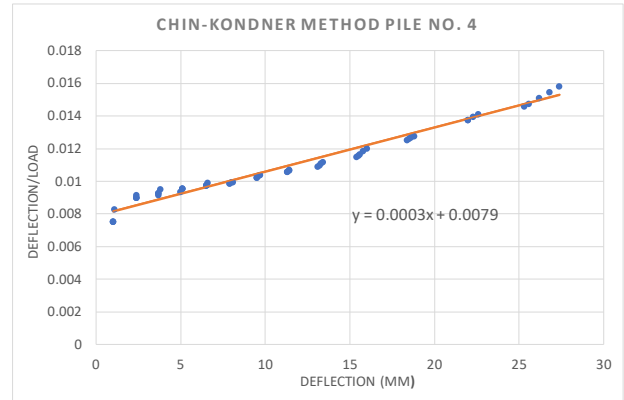


Figure A18. Chin-Kondner Extrapolation Method Pile No. 4

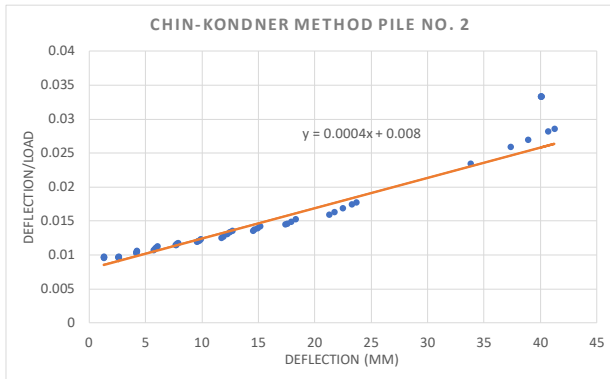


Figure A16. Chin-Kondner Extrapolation Method Pile No. 2

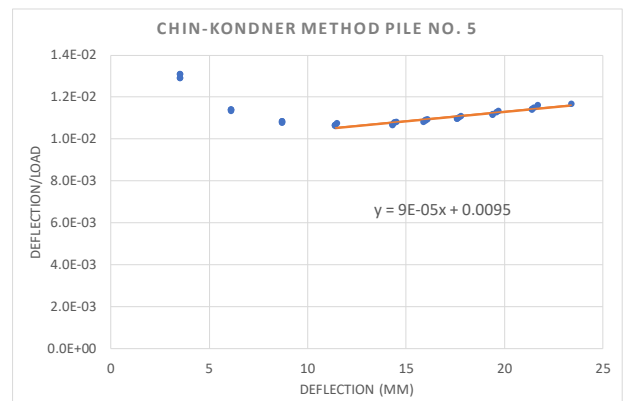


Figure A19. Chin-Kondner Extrapolation Method Pile No. 5

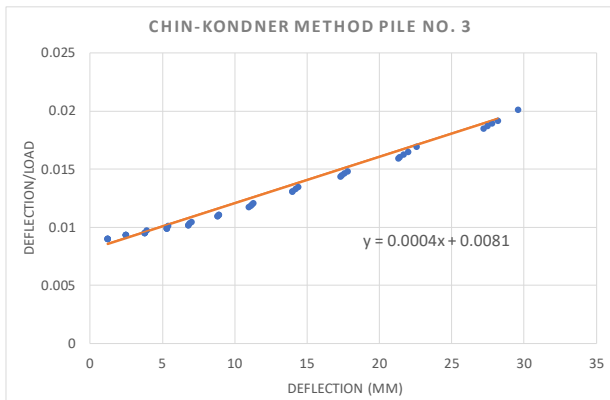


Figure A17. Chin-Kondner Extrapolation Method Pile No. 3

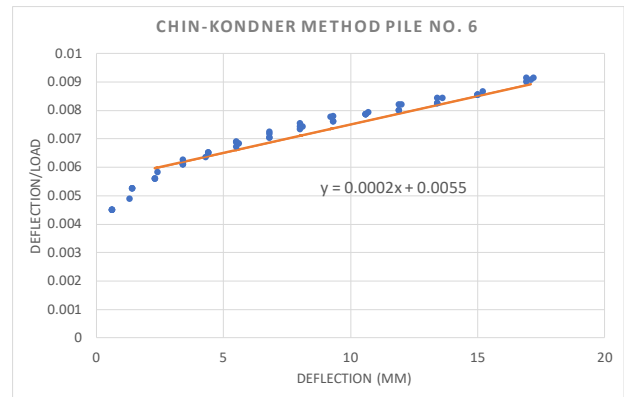


Figure A20. Chin-Kondner Extrapolation Method Pile No. 6

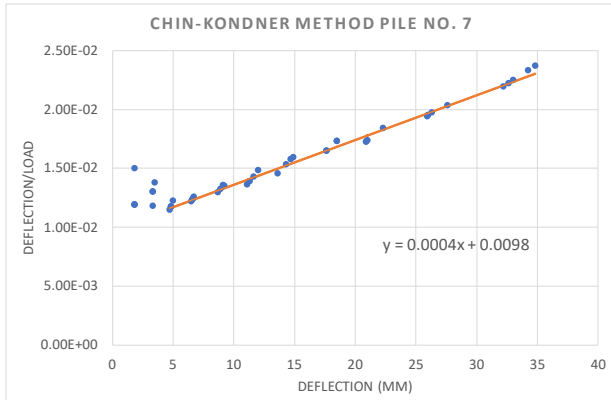


Figure A21. Chin-Kondner Extrapolation Method Pile No. 7

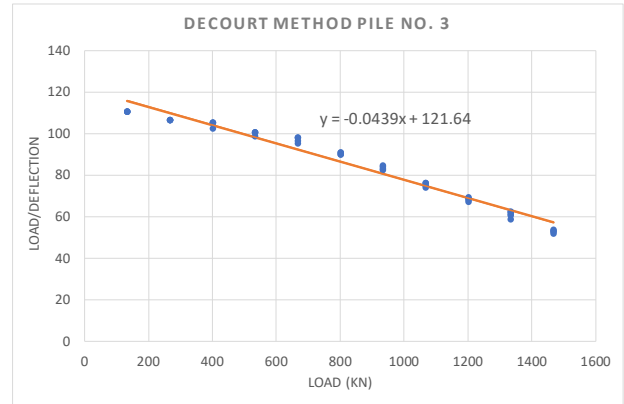


Figure A24. Decourt Extrapolation Method Pile No. 3

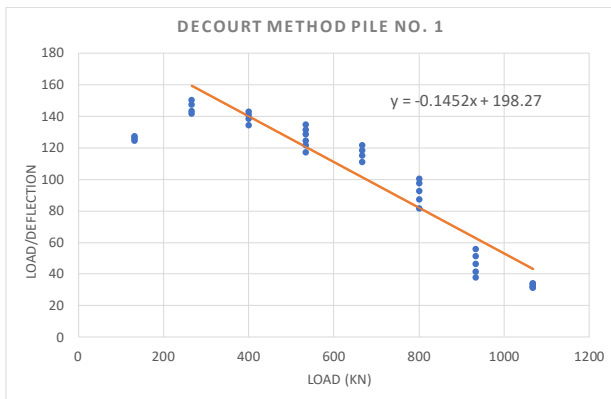


Figure A22. Decourt Extrapolation Method Pile No. 1

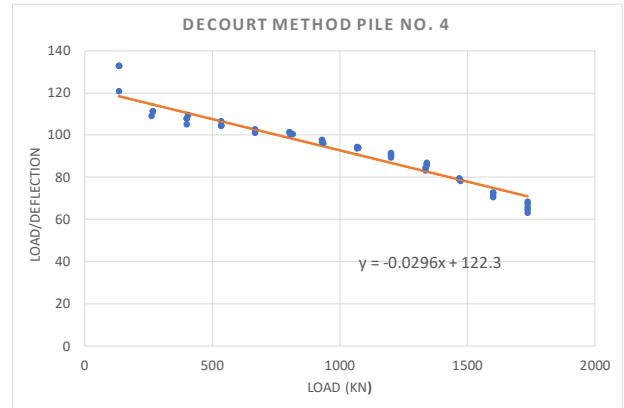


Figure A25. Decourt Extrapolation Method Pile No. 4

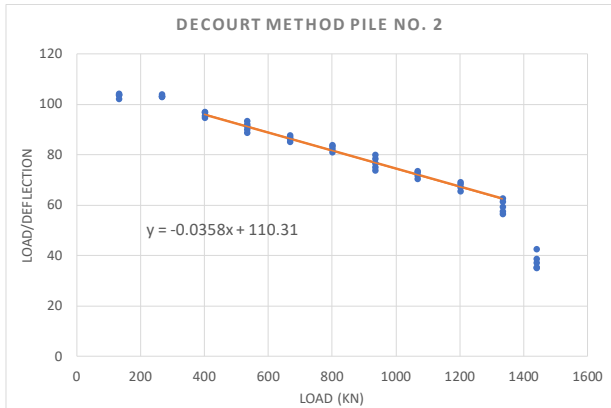


Figure A23. Decourt Extrapolation Method Pile No. 2

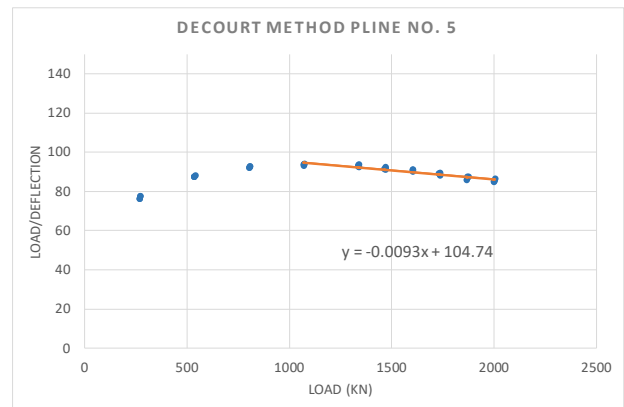


Figure A26. Decourt Extrapolation Method Pile No. 5

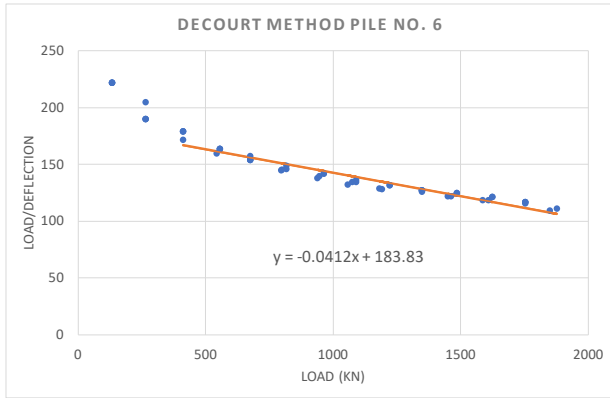


Figure A27. Decourt Extrapolation Method Pile No. 6

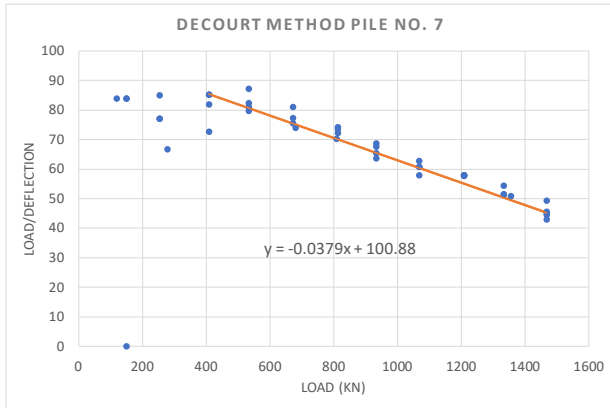


Figure A28. Decourt Extrapolation Method Pile No. 7

APPENDIX B

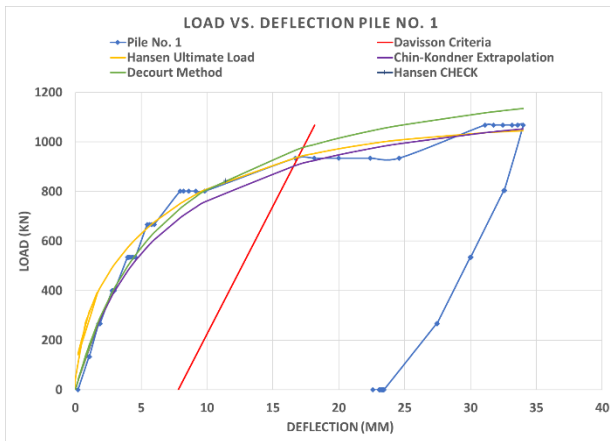


Figure B1. Summary of Pile Load Test Analysis Pile No.1

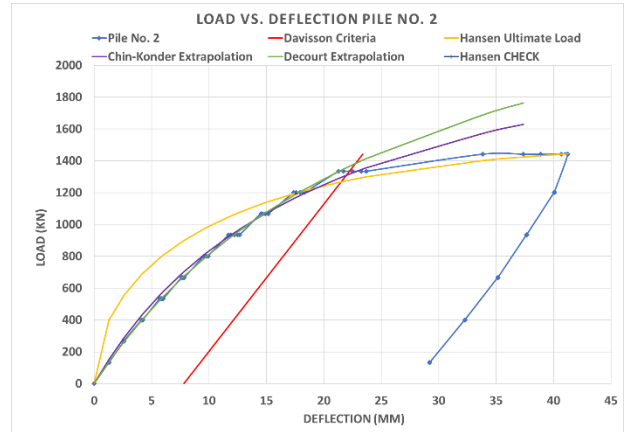


Figure B2. Summary of Pile Load Test Analysis Pile No.2

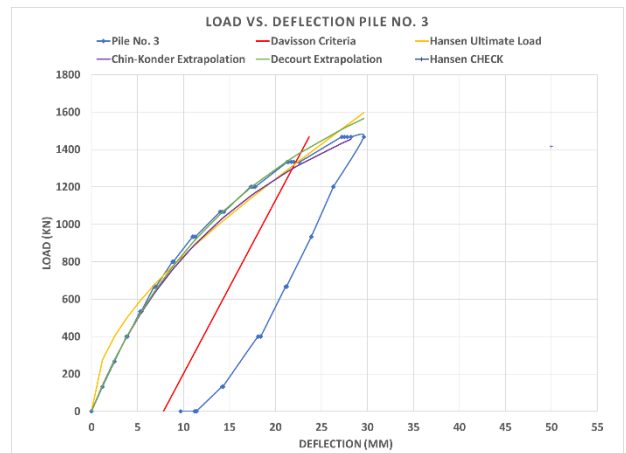


Figure B3. Summary of Pile Load Test Analysis Pile No.3

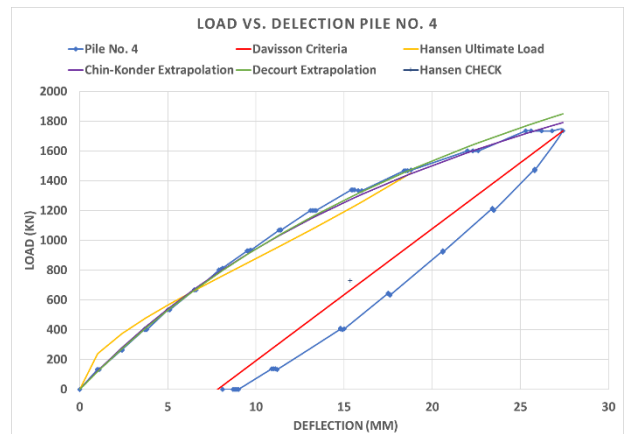


Figure B4. Summary of Pile Load Test Analysis Pile No.4

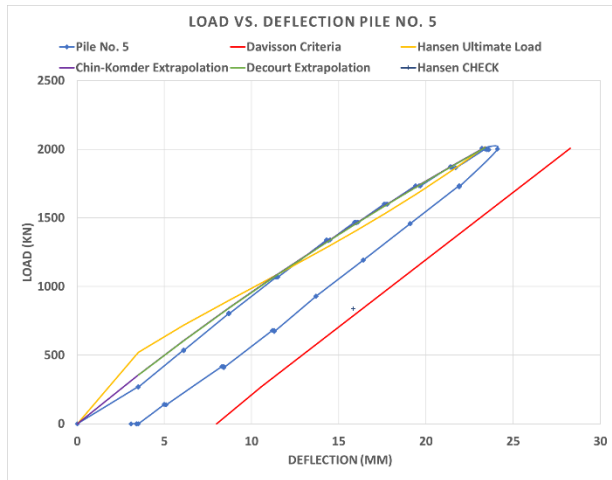


Figure B5. Summary of Pile Load Test Analysis Pile No.5

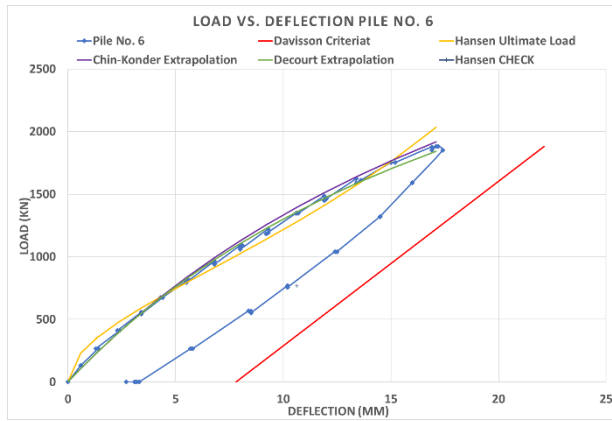


Figure B6. Summary of Pile Load Test Analysis Pile No.6

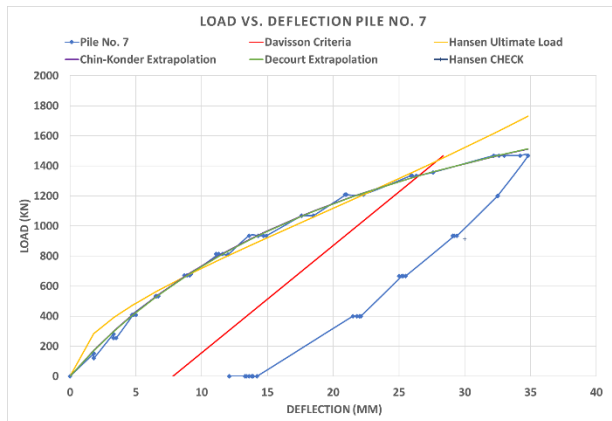


Figure B7. Summary of Pile Load Test Analysis Pile No.7